Chemistry–A European Journal
Research Article
doi.org/10.1002/chem.202303343
Chemistry Europe
European Chemical Societies Publishing
www.chemeurj.org

Oligo-Condensation Reactions of Silanediols with Conservation of Solid-State-Structural Features

Jan-Falk Kannengießer,[a] Bernd Morgenstern,[a] Oliver Janka,[a] and Guido Kickelbick*[a]

Oligo- and polysiloxanes are usually prepared by condensation reactions in solvents without control of stereochemistry. Here we present a solventless thermal condensation of stable organosilanols. We investigated the condensation reactions of organosilanediols with different organic substituents, having in common at least one aromatic group. The condensation kinetics of the precursors observed by NMR spectroscopy revealed a strong dependence on temperature, time, and substitution pattern at the silicon atom. SEC measurements showed that chain length increases with increasing condensation temperature and time and lower steric demand of the substituents, which also influences the glass transition temperatures (T_g) of the resulting oligo- or polymers. X-ray diffraction studies of the crystalline silanediols and their condensation products revealed a structural correlation between the substituent location in the crystalline precursors and the formed macromolecules induced by the hydrogen bonding pattern. In certain cases, it is possible to carry out topotactic polymerization in the solid-state, which has its origin in the crystal structure.

Introduction

Polysiloxanes are an important polymer class due to their high optical transmission in combination with an adjustable refractive index (RI), their thermal stability, and their chemical inertness in combination with other features such as tuneable mechanical properties.[1] For many of the applications the polymers are applied as 2-component thermosets, with linear polysiloxanes being the starting materials.[2–5] The macromolecules are usually prepared by polycondensation reactions from dichloro- or dialkoxysilane precursors, which are typically hydrolyzed in an acid-catalyzed reaction followed by an immediate condensation of the commonly unstable silanol intermediates (Scheme 1a).[6] In the acid catalysed reaction, condensation proceeds quite slowly, resulting in the hydrolysis being the rate-determining step.[7] Hence, the polycondensation is a kinetically controlled process, which often reaches an equilibrium state in which linear chains and rings are the products. The ratio between these two species can be influenced by the reaction conditions, such as temperature, pH, or precursor concentration.[8] From a synthetic point of view, it would be advantageous if the hydrolysis of the precursors could be separated from their condensation (Scheme 1 b), which could also lead to better control of the properties of the resulting polymers. A prerequisite for this is the possibility of isolating stable silanols as precursors and then condensing them separately.

The stability and therefore the condensation of silanols is significantly related to the chemical environment of the silicon atom, as this affects the acidity of the silanol group and also the strength of the hydrogen bonds of the molecular precursors, which in turn affects the condensation reaction.[9–11] Generally, electron-withdrawing substituents have an advantageous effect for rapid condensation, since the silicon atom becomes more electrophilic and can thus be attacked more easily by the Si-OH groups.[12] As in other substitution reactions, the sterical environment at the silicon center to be attacked also plays a major role in the reactivity.[13] The reaction environment and the substitution pattern at the silicon atoms also influences the properties of the resulting oligo- and polysiloxanes, such as the glass transition temperature (T_g)[14–18] or the RI.[19–20]

Different stable monosilanols, silanediols and -triols are already described in literature, such as Ph_3SiOH,[21] Et_3SiOH,[21] $(n\text{-Bu})_3SiOH$,[21] $(tert\text{-BuO})_3SiOH$,[22] $Me_2Si(OH)_2$,[23] $Ph_2Si(OH)_2$,[24] $(cis\text{-}C_6H_{11})_2Si(OH)_2$,[25] $(tert\text{-Bu})_2Si(OH)_2$,[10] $(ortho\text{-tolyl})_2Si(OH)_2$,[26] $(iso\text{-propyl})_2Si(OH)_2$[27] $PhSi(OH)_3$,[28] $c\text{-}C_6H_{11}Si(OH)_3$[29–30] and $tert\text{-BuSi(OH)}_3$.[31] Silanediols have been already used, for example, in the synthesis of LED encapsulation resins and in pharmaceutical applications,[24,32–33] monosilanols were applied as catalysts for various organic syntheses, such as cross coupling reactions[34–36] or direct amidation of carboxylic acid[37] and silanetriols have already been used for the synthesis of various metallasiloxanes[38–39] and POSS cages.[40–42]

Many of the stable silanols are solid and crystalline at room temperature. Due to the high acidity and simultaneous basicity of the silanol group, silanols can form very strong hydrogen bonds, significantly stronger than those of comparable carbinols.[10,38] In their crystal structures, the hydrogen bonds result very often in specific patterns, especially in the case of

[a] J.-F. Kannengießer, Dr. B. Morgenstern, Priv. Doz. Dr. O. Janka, Prof. Dr. G. Kickelbick
Saarland University, Inorganic Solid-State Chemistry,
Campus, Building C4 1, 66123 Saarbrücken, Germany
E-mail: guido.kickelbick@uni-saarland.de
Homepage: https://www.uni-saarland.de/lehrstuhl/kickelbick.html

Supporting information for this article is available on the WWW under https://doi.org/10.1002/chem.202303343

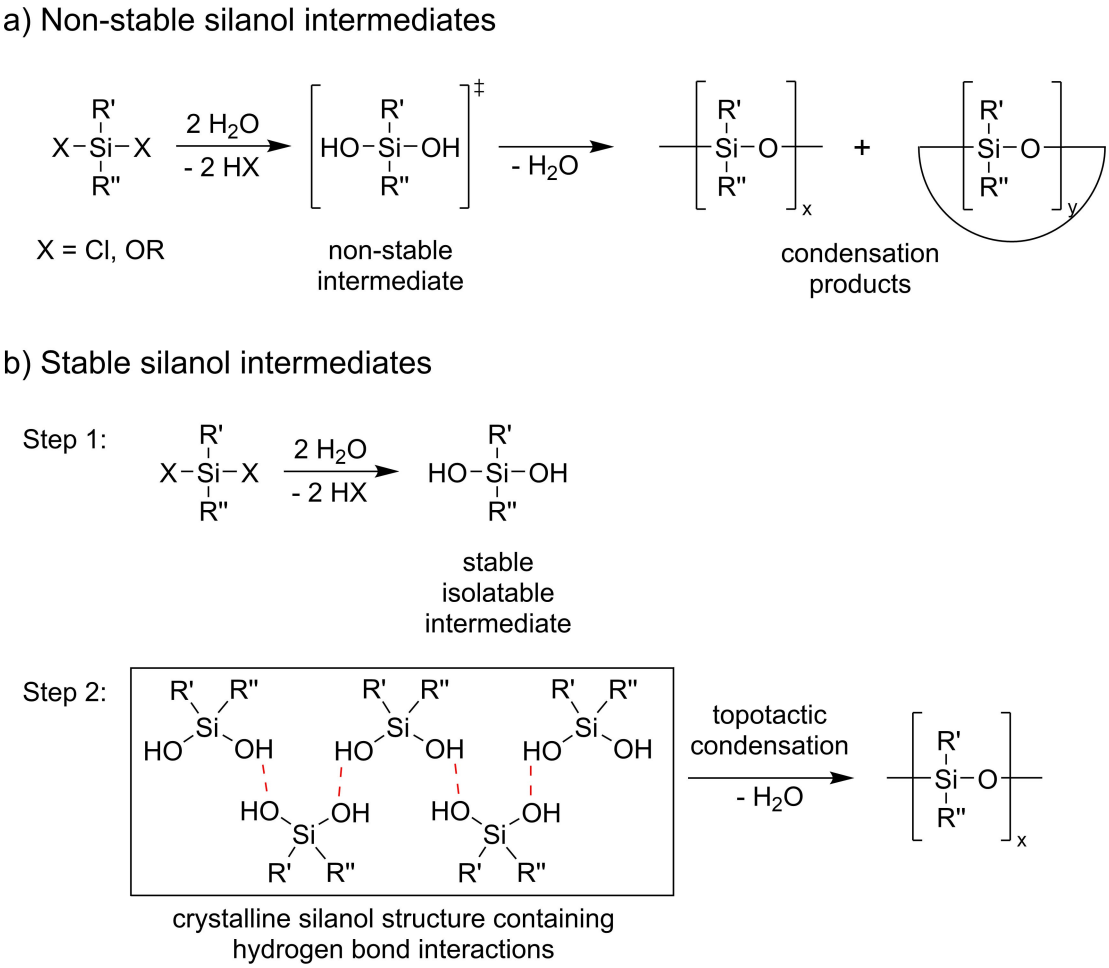

Scheme 1. Difference between condensation of non-stable silanol intermediates (a) and stable silanol molecules (b).

silanediols.[10–11,38] In contrast, in case of monosilanols isolated groups are more common in the solid-state, due to the three often steric demanding substituents.[10,38]

The hydrogen bonding patterns in solid silanols can be advantageous for condensation reactions and the formation of oligo- or polymers in the solid-state. Particularly the pre-orientation in their crystal structures can result in a control of tacticity if the oligo- and polymers can be formed in a mild topotactic reaction.[43] Such so called solid-state polymerizations (SSP) are also ecologically interesting because they do not require organic solvents. For this type of polymerization, the condensation barrier usually has to be overcome by a thermal process. The potential topotactic polymerizations can yield products with properties that cannot be obtained under solvent-based conditions.[44–47] Up to now, no example of a controlled silanol polycondensation starting from stable silanols has been reported in the solid-state. In view of reducing the use of organic solvents and thus introducing more environmentally friendly processes, SSP starting with stable silanols could provide an alternative method to conventional polymerization processes.

In previous studies, we observed a high stability of silanols when polycyclic aromatic substituents are used at the silicon atom.[11] These aromatic groups seem to particularly stabilize the formation of stable silanols. The aim of this work was the synthesis of stable isolable aryl-substituted silanediols and the investigation of their thermal condensation in the solid-state. Particularly we studied the activation barrier for the condensation process and the parameters that favour the condensation behaviour in the solid-state.

Previously studied condensation reactions of monosilanols in solution revealed a strong dependence of the condensation rate on the substituents on the silicon. Thus, a higher steric demand of a substituent resulted in a strongly reduced condensation rate.[13] Furthermore, the condensation reaction of silanediols in solution revealed a two-step process caused by the sterical demand near the active silanol groups.[48] The condensation of silanetriols has also been investigated in the literature.[39,41–42, 49–50] These are particularly suitable for the formation of discrete components, such as POSS cages[42] or metallasiloxanes.[39,51] The reactivity of silanetriols is also largely determined by the substituents on the silicon and their steric influence.[41] Silanetriols are generally the most unstable representatives of the silanol class and usually condense in solution at room temperature.[41,49] John F. Brown showed that the condensation of phenylsilanetriol is not really random, but

takes place according to a certain pattern.[50] The same intermediates are always observed and linear structures are preferred at the start of condensation, with ring structures being formed afterwards if possible. However, our goal was the investigation of the reaction in the solid-state, as topotactic reaction control should work best in the solid-state, due to the pre-orientation of the molecules. In general, two temperature ranges can be distinguished for thermally induced condensation: (I) the temperature below the melting point, at which the entire system is still in the solid-state, and (II) the temperature around or above the melting point, at which a reaction behaves more like condensation in solution because the molecules are free to move. For a condensation reaction to occur below the melting point only small reorientations of the molecules in the solid are sufficient to initiate the condensation reaction. This means that in the solid-state the molecules are ideally oriented in such a way that hydrogen bonds between the Si-OH groups are already formed. A number of X-ray single crystal structures of monosilanols are known to literature,[52–59] including the structure of triphenylsilanol[52,55–57] or dimethyl(naphthalen-1-yl)silanol (this work, Figure S1). In several crystal structures, a preorientation of the silanols is observed, which might be advantageous for a solid-state condensation. In other cases such a preorientation is not present,[10,38] which leads to the necessity that the entire molecules must move for the condensation reaction taking place. Below the melting point, a condensation reaction is therefore often hardly possible.

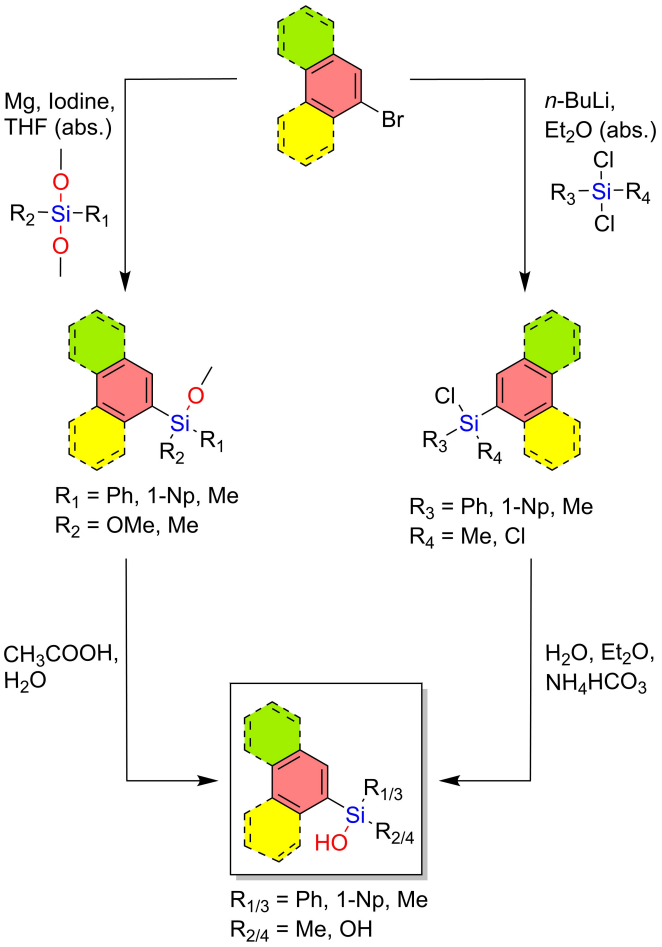

Scheme 2. Synthesis of aromatic alkoxy- or chlorosilanes and subsequent hydrolysis to form mono- and silanediols.

Results and Discussion

The aim of our study was the investigation of the thermal topotactic condensation reaction of silanediols without solvent in the solid-state or alternatively in the melt. If not commercially available, the silanediols were prepared from the respective alkoxy and chlorosilane precursors by Grignard or organolithium reactions.[11] Subsequent hydrolysis was realized by addition of water in presence of an acid scavenger (NH_4HCO_3) for the chlorosilane precursors or with highly diluted acetic acid for the alkoxysilanes (Scheme 2).

Thermal condensation of silanediols

Contrary to the condensation reaction of the monosilanols, which results in dimers, silanediols can deliver linear or cyclic oligo- or polysiloxanes[60] as reaction products (Scheme 3). In this case, the linear oligomers have silanol groups at the ends, which allows the oligomers to condense further. The corresponding single crystal structures of the investigated silanediols, which were all solid at room temperature, are shown in the Supporting Information (Figures S6–S9). The silanol group hydrogen bonding patterns can be easily identified in these crystal structures. $Ph_2Si(OH)_2$ plays an outstanding role because it is commercially available and was already used in several solvent based studies in the literature, for example, in the formation of siloxane based materials.[61–66] However, no study of the thermal condensation behavior in the solid-state was reported yet. The melting point of $Ph_2Si(OH)_2$ determined by the peak maxima in DSC is in the temperature interval 155–160 °C. According to the literature, it starts to melt at approx. 140 °C.[67] Therefore, the temperature interval between 120 °C and 180 °C was chosen to study the condensation kinetics in the solid as well as in the molten state (Figure 1). The melting points of the other investigated silanediols can be found in the supporting information (Table S1).

The solid-state condensation for diphenylsilanediol for different condensation temperatures was studied by ^{1}H NMR spectroscopy in an aceton-d_6 solution integrating the total silanol groups. For this purpose, the solid samples were heated in defined amounts without any solvent in a sealed NMR tube under ambient conditions, after certain time intervals, the NMR tubes were removed from the heating bath, and NMR solvent was added before measurement. We observed a temperature-dependent decrease in the integral of the silanol OH signal, indicating a rather slow condensation reaction at 120 °C with about 6% conversion of the silanol groups after 90 minutes (Figure 1). At 180 °C, considerably above the melting point, a conversion of 75 % of the silanol groups was detected after the same time. A temperature just below the melting point at

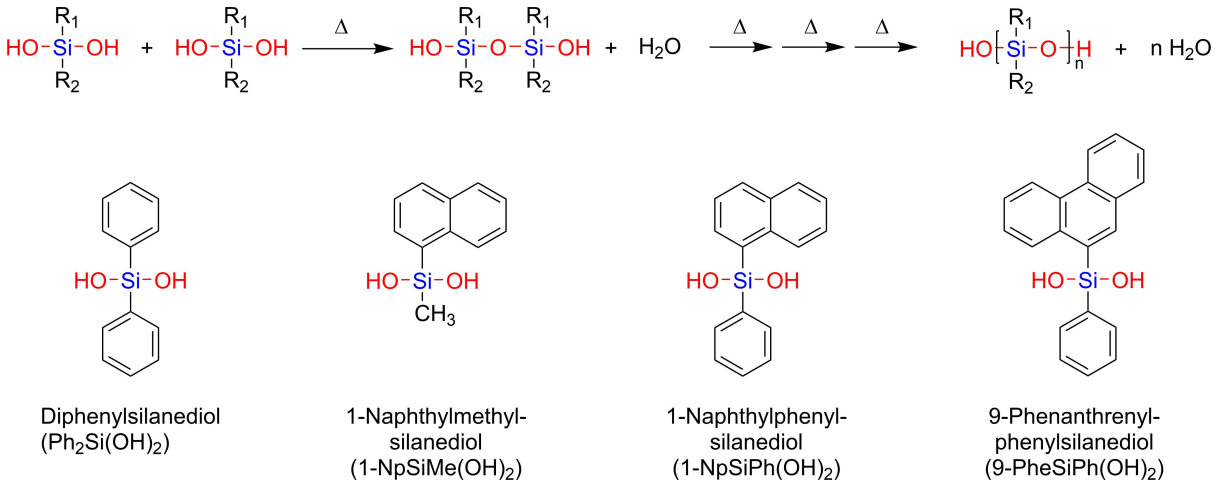

Scheme 3. Thermally induced condensation of silanediols and the studied compounds.

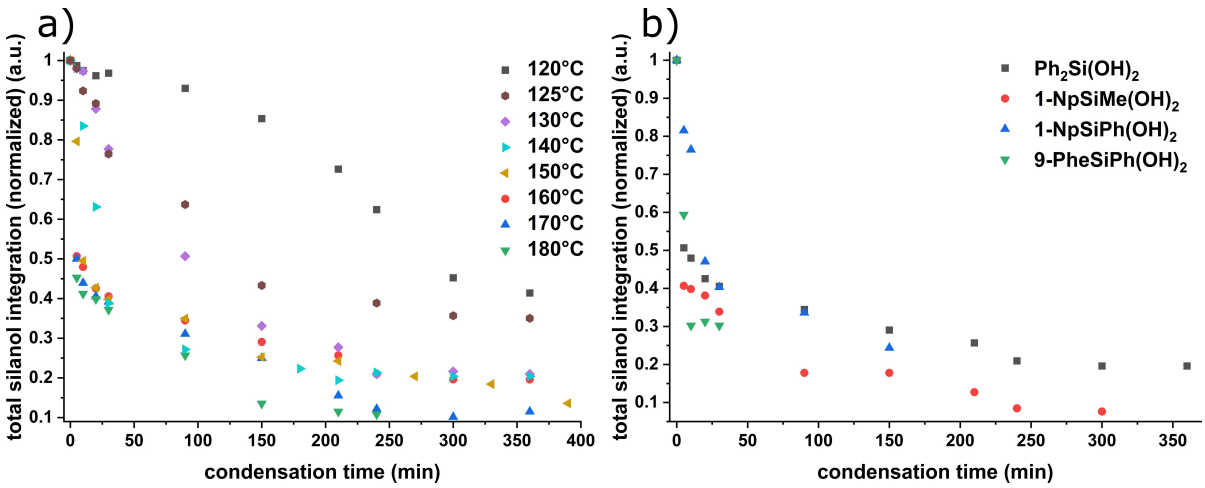

Figure 1. a) Integrations of all ^{1}H NMR silanol signals of $Ph_2Si(OH)_2$ as a function of condensation time at temperatures from 120 °C-180 °C. b) Normalized total silanol integration upon thermal treatment at 160 °C of $Ph_2Si(OH)_2$, 1-NpSiMe$(OH)_2$, 1-NpSiPh$(OH)_2$, and 9-PheSiPh$(OH)_2$. For 1-NpSiPh$(OH)_2$ and 9-PheSiPh$(OH)_2$, no reasonable integration could be determined at later time points because the silanol signals were overlaid by the signals of the aryl substituents.

140 °C (around 70% conversion after 90 min) seems to be an optimum for the solid-state condensation and should therefore also be ideal for a potentially topotactic reaction. As expected, a condensation in the molten state is considerably faster and the reaction rate increases with increasing temperature (Figure 1a). The general condensation process was comparable at all temperatures, except at 120 °C, where condensation is much slower and slightly different kinetically. However, it was also shown that temperatures well below the melting point of the compound (e.g., 130 °C) can be sufficient for condensation. The thermal condensation seems to have almost reached its maximum (at least 80% conversion at all temperatures) after approximately 4 h. In a later chapter, which will deal with aryl cleavage in silanols it was also shown that the lowest possible condensation temperature is desirable to suppress aryl cleavage.

The thermal condensation was furthermore investigated with respect to substituents at the silicon atom, which can have a crucial influence on the condensation rate of silanediols, for example, due to the steric influence of the groups. We have chosen 160 °C as the temperature for this study. Although this temperature is above the melting point of the compounds and we therefore cannot postulate a pure solid-state polymerization, it is required to obtain a sufficiently fast condensation for all studied silanediols. The comparison of the total silanol integration (Figure 1b) shows a similar course for the compounds investigated. Within the first 10 minutes (for 1-NpSiPh$(OH)_2$ and 9-PheSiPh$(OH)_2$, no reasonable integration could be determined at later points in time because the signals of new formed silanols groups were overlaid through broadening aryl signals), the following order of reaction rates can be identified: 1-NpSiPh$(OH)_2$ < 9-PheSiPh$(OH)_2$ < 1-NpSiMe$(OH)_2$ < $Ph_2Si(OH)_2$. A general correlation can be established between the substituents on the silicon and the reaction rates: Compounds with smaller organic substituents exhibit higher reaction rates. 9-PheSiPh$(OH)_2$, however, does not quite fit this picture as it exhibits a higher condensation rate compared to 1-NpSiPh$(OH)_2$, although it is sterically much more demanding

with the larger phenanthrenyl substituent. In the case of 1-NpSiMe(OH)$_2$ and Ph$_2$Si(OH)$_2$, it is arguable which of the two is sterically more demanding, since 1-NpSiMe(OH)$_2$ has a naphthyl substituent but also a small methyl substituent, whereas Ph$_2$Si(OH)$_2$ has two phenyl substituents.

^{29}Si NMR spectra of the compounds at selected condensation conditions (4 h at 150 °C) showed the existence of D^2 (–O-SiR$_2$-O > C- >) and D^1 (–O-SiR$_2$-OH) units for all compounds. Thus, both chain units and chain ends are present in the products (Figures S10–S13). The occurrence of ring structures cannot be excluded with this method.

To further support the ^{1}H NMR study, we repeated the study using ^{29}Si NMR spectroscopy (Figure 2). ^{29}Si NMR has two fundamental disadvantages compared to ^{1}H NMR spectroscopy: (i) because of the significantly longer measurement times the sample can change within the NMR tube by ongoing condensation reactions, which is why we reduced the relaxation time applying chromium(III) acetylacetonate as relaxation agent. (ii) Due to the significantly lower relative abundance of the ^{29}Si isotope, considerably more sample (100 mg) had to be used to improve the signal-to-noise ratio. The study itself was again carried out with the samples in closed NMR tubes that were heated in an oil bath. Due to the long NMR measurement times, some samples could not be measured immediately. In these cases, the sample was removed from the oil bath and immediately frozen until a measurement was possible. The NMR spectra were analysed by integrating all signals and relating the original monomer signal to the sum of all integrals. This allows the remaining fraction of the original monomer to be determined, which should decrease during condensation. It should be noted that the ^{29}Si NMR study can partially support the ^{1}H NMR study, but the two studies provide different information. The ^{29}Si NMR study only shows the percentage of the monomer and is finished when the monomer has been completely consumed. However, the condensation itself is not yet complete, as various oligomers with still active and condensable silanol groups are now present. In contrast, in the ^{1}H NMR study all silanol groups and thus also different oligomers can be detected. In this case, the condensation can therefore be observed beyond the complete consumption of the monomer.

The obtained kinetics of the two studies are partially comparable, especially at temperatures above 140 °C. At these temperatures, the ^{29}Si NMR study (Figure 2) shows, as expected, a faster consumption of the monomer compared to the total consumption of the silanol groups (Figure 1). However, at 120 °C, 125 °C and 130 °C large differences can be observed. The ^{29}Si NMR study (Figure 2a) shows a much slower disappearance of the original Ph$_2$Si(OH)$_2$ than would be expected from the ^{1}H NMR study (Figure 1a). This could be related to the lower sensitivity of the ^{29}Si NMR study, as different species that are already present in reality may not be seen and therefore cannot be integrated. Furthermore, the signal-to-noise ratio was significantly worse than in ^{1}H NMR spectroscopy despite the use of a relaxation agent and a larger amount of sample.[68] This makes it more difficult to analyze the resulting products, especially if they are formed very slowly and in small quantities due to the lower condensation temperature. This reduces the overall integration of all silicon compounds, which increases the proportion of the remaining monomer.

A comparison of the condensation behavior of the different silanediols at the same temperature (Figure 1b and Figure 2b) shows a similar pattern. The result of the analysis shows that the monomer is consumed much faster than the silanol groups as a whole. The comparatively slower consumption of 1-NpSiPh(OH)$_2$ is remarkable, but no real conclusions can be drawn from this relative to the ^{1}H NMR study, as the slower monomer consumption can be explained by a slightly different condensation behavior. For example, it is possible that although condensation is fast in all compounds, in 1-NpSiPh(OH)$_2$ the oligomeric structures tend to condense with each other and thus the monomer is retained a little longer in some cases.

Thermogravimetric studies at a given isotherm should also allow conclusions about thermal condensation, since the condensation of silanols produces water, which volatilizes at the conditions studied here and is thus responsible for a mass

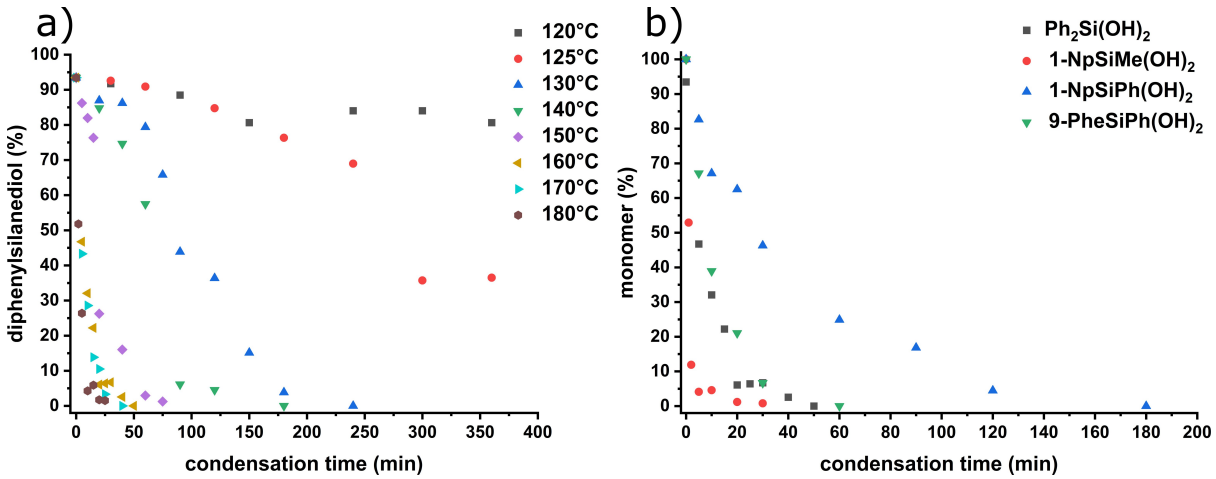

Figure 2. a) Monomer content, determined by ^{29}Si NMR of Ph$_2$Si(OH)$_2$ as a function of condensation time at temperatures from 120 °C-180 °C. b) Monomer content, determined by ^{29}Si NMR upon thermal treatment at 160 °C of Ph$_2$Si(OH)$_2$, 1-NpSiMe(OH)$_2$, 1-NpSiPh(OH)$_2$, and 9-PheSiPh(OH)$_2$.

loss. When examining the condensation process by thermogravimetry (Figure 3a), a very similar course to the NMR study shown above is noticed. The mass loss is caused by the water produced during the condensation process and benzene which is released through Si–C bond cleavage, especially at higher temperatures. It is interesting to note that a two-stage process is observed at temperatures below 160 °C and a three-stage process at higher temperatures. In all these steps, condensation occurs with consumption of the silanol groups and thus also elimination of water. This was already shown in the NMR study above. Only the rate of water loss seems to differ during condensation, which is expressed in the different processes with different slopes. Unfortunately, it is difficult to determine the exact conversion by gravimetry since benzene is split off especially at higher temperatures. This phenomenon will be further investigated later. When comparing the different silanediols at a condensation at 160 °C gravimetrically, no real trend can be observed (Figure 3b). However, what all the results have in common is that there is a rapid mass loss at the beginning which then levels off. Interestingly, 9-PheSiPh(OH)$_2$ shows an almost linear mass loss over the observed time. This compound also shows the highest mass loss, which can probably be explained by a cleavage of other by-products (*vide infra*).

The average molar mass after the condensation reaction can be an indicator for the completeness of the reaction, even if a low molecular mass does not necessarily mean that the condensation is less advanced. The degree of condensation can be determined by a combination of NMR and SEC studies. On the other hand, in condensation reactions of silanols two products can form, linear chains and ring systems. We applied two different methods to investigate the molecular weight of the resulting products, namely size exclusion chromatography (SEC) and FT-ICR mass spectroscopy. The model Ph$_2$Si(OH)$_2$ was investigated with respect to the influence of the condensation time. The corresponding molecular mass distributions can be found in the Supporting information (Figures S14-S19). SEC analysis showed that oligomeric products were formed rather than polymers. Since these oligomers are silanol terminated, further condensation is possible.

During the thermally induced condensation process of Ph$_2$Si(OH)$_2$, a steadily increasing molar mass is noticeable, which, however, is relatively small with about 350–1050 g mol^{-1}. Thus, smaller oligomers with a chain length of 2–6 units are most likely present. Over time the molar mass increases with a similar time dependency as observed in the NMR study (Figure 4a). The polydispersity decreases at the beginning, but then increases again continuously. To just briefly show a temperature dependence, additional molecular masses were determined at different condensation temperatures exclusively for Ph$_2$Si(OH)$_2$ (Figure 4b). As expected, it was found that a higher temperature leads to a higher molecular mass. In addition, the molecular weights of the condensation products of the other silanediols were determined at a specific condensation point (150 °C; 4 h) (Figure 4b). There, the highest molecular weight was shown for compound 1-NpSiMe(OH)$_2$, which can be explained by the quite small methyl groups that allow a less sterically demanding condensation process. Compounds 1-NpSiPh(OH)$_2$ and 9-PheSiPh(OH)$_2$, which have large aryl substituents, have the lowest molecular weights. The FT-ICR MS measurements are consistent with the results of the SEC. Oligomers with a size of 3–8 repeating units were also found there (Figures S20–S22).

The same samples used for SEC were also analyzed by DSC to investigate the T_g of the resulting oligo- or polymers (Figures S23-S26). Within the first 6 h of the condensation reaction, T_gs kept quite constant. Within 24 h of condensation, the T_g increased, but remained relatively constant thereafter (Figure 4a). This trend follows the literature known increase of T_g with increasing condensation molecular weight.[69]

The T_g at different condensation temperatures was determined for the condensation products of compound Ph$_2$Si(OH)$_2$ (Figure 5b). An increase of the T_g correlates with a higher condensation temperature and a longer chain length (Figure 4b). Again, the other silanediols were examined at a specific point in the condensation (150 °C; 4 h) with respect to their T_g

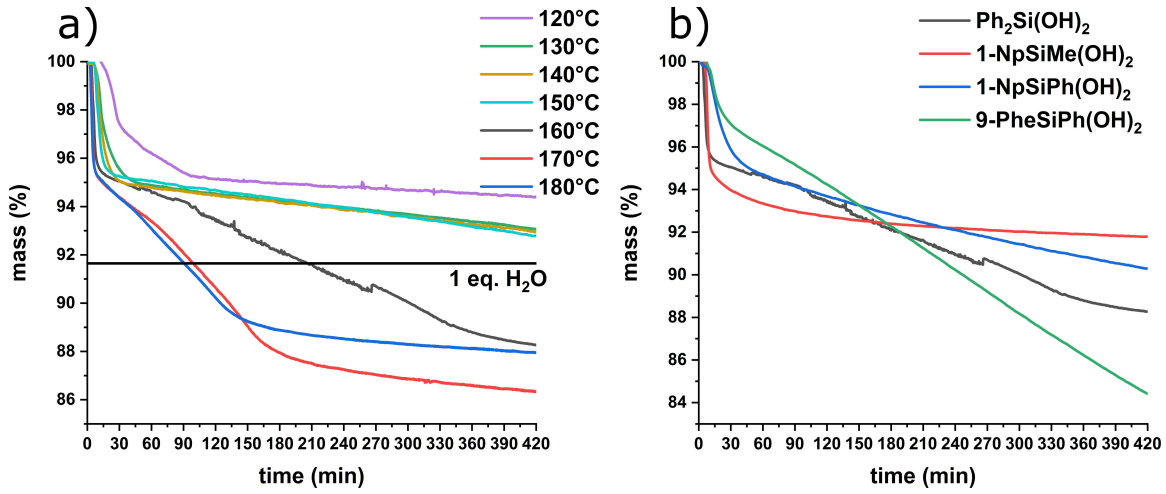

Figure 3. a) Gravimetric study of the thermal condensation of diphenylsilanediol (Ph$_2$Si(OH)$_2$) at different temperatures. b) Comparison of the gravimetric behavior of silanediols Ph$_2$Si(OH)$_2$, 1-NpSiMe(OH)$_2$, 1-NpSiPh(OH)$_2$, and 9-PheSiPh(OH)$_2$ during condensation at 160 °C.

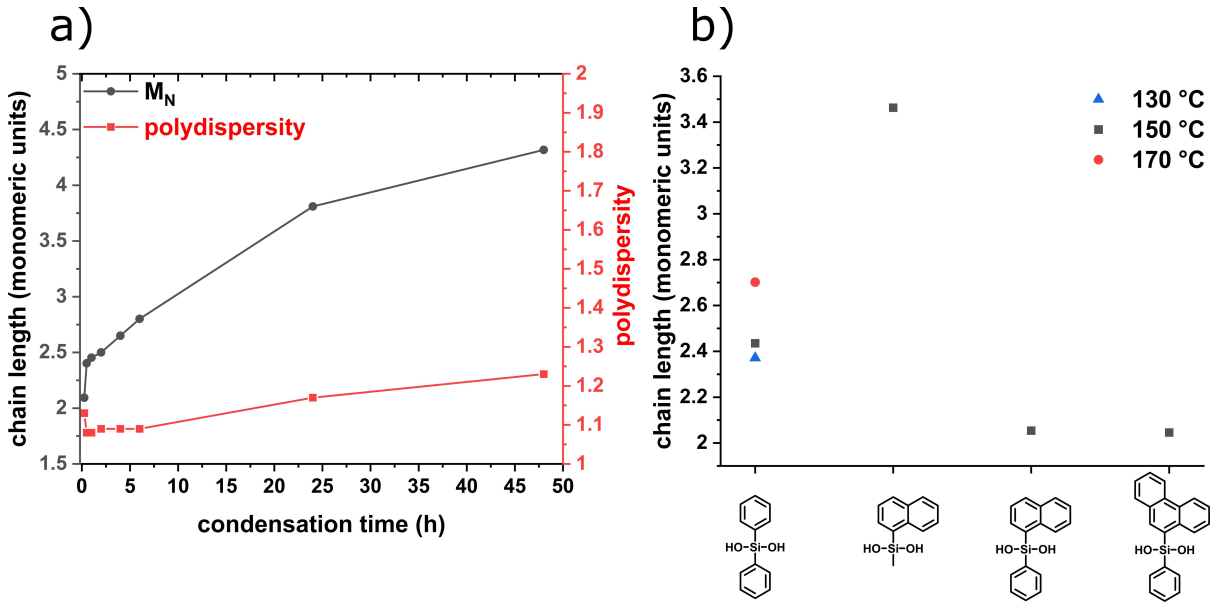

Figure 4. a) Development of the molecular weight and polydispersity during the condensation of $Ph_2Si(OH)_2$ at 150 °C. b) Comparison of molecular weight at different condensation temperatures for $Ph_2Si(OH)_2$ and comparison of different precursor compounds at 150 °C condensation temperature for 4 h condensation time.

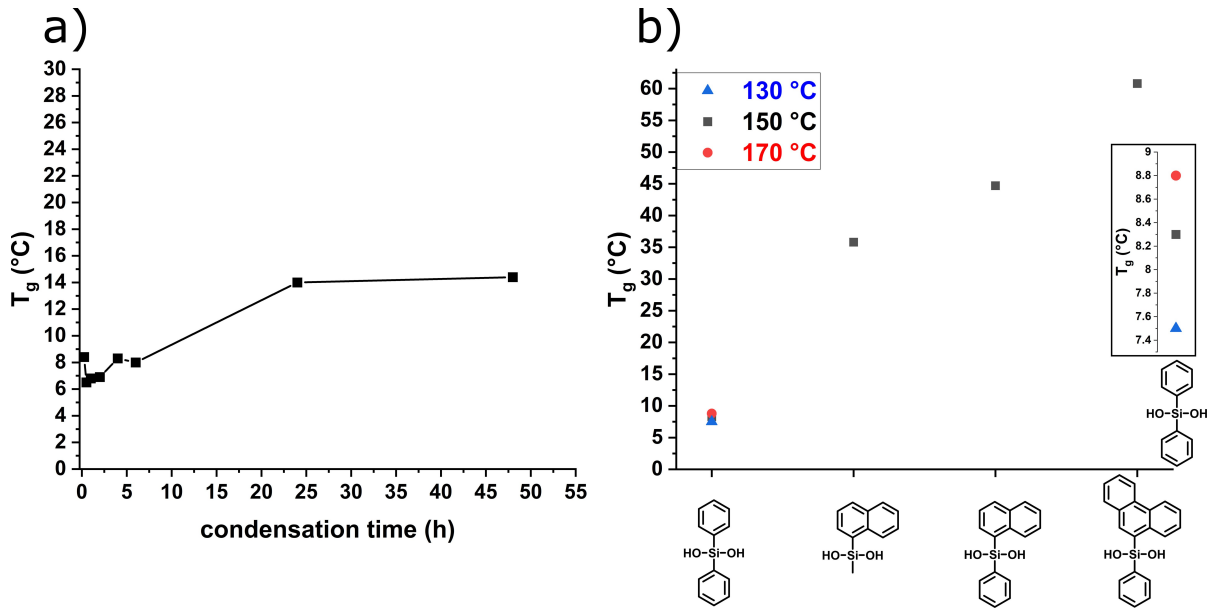

Figure 5. a) Time dependent development of the T_g during the condensation of $Ph_2Si(OH)_2$ at 150 °C. b) Comparison of the T_g at different condensation temperatures for $Ph_2Si(OH)_2$ and comparison of different precursor compounds at 150 °C after 4 h.

(Figure 5b). As expected, the T_g correlates in this study with the sterical demand of the substituents at the silicon atom. The steric influence of the substituent seems to be even stronger than the influence of the chain length, since the condensation products of compounds 1-NpSiPh(OH)$_2$ and 9-PheSiPh(OH)$_2$ show significantly higher T_gs, despite the lower chain length. This is probably due to the fact that the difference between the chain lengths is comparatively low, since only oligomers are present in all condensation products.

By-products of thermal condensation

TG-MS coupling was used to detect the molecules split off during condensation and to correlate them with the corresponding mass losses. Figure 5a shows the result of the TG-MS coupling for $Ph_2Si(OH)_2$. The measurements of the other silanediols can be found in the supporting information (Figures S29). The first mass loss can be correlated exclusively with the elimination of water. Interestingly, two maxima are detected in this splitting. The second mass loss can be

correlated on the one hand with a renewed splitting off of water and on the other hand with a splitting off of benzene. Unfortunately, this method cannot really be used for quantification because the separations within the temperature program are not completely finished. In addition, for the silanediols that have larger aryl substituents (1-NpSiMe(OH)$_2$, 1-NpSiPh(OH)$_2$ and 9-PheSiPh(OH)$_2$), it cannot be guaranteed that the aromatic fragments, i.e., naphthalene and phenanthrene, are completely transported to the mass spectrometer due to their high boiling points.

To study the by-products in another way and also quantitatively, a reaction setup was used, in which the sample is heated for three hours using an oil bath. The volatile compounds formed during condensation are transferred by a stream of argon through a short PTFE cannula into a second small glass vessel containing an appropriate NMR solvent, i.e., acetone-d$_6$ (Figure S30). The cannula on the NMR solvent side is immersed in the solvent to dissolve the resulting compounds. To prevent the solvent from evaporating, the collecting vessel was placed in an ice bath. The temperature used for the study was set to 20 °C above the melting temperature, as determined by DSC. To study the condensation in this way, both the condensate was analyzed by ^{1}H NMR spectroscopy using vinyltrimethoxysilane as an internal standard and ^{13}C NMR spectroscopy, and the remaining condensation product in the distillation sump was analyzed by ^{1}H and ^{29}Si NMR spectroscopy.

The elimination of benzene, naphthalene and phenanthrene was demonstrated by the detection of the corresponding signals of the free molecules in the condensate with ^{1}H and ^{13}C NMR spectroscopy. A significant aryl cleavage only occurs above 150 °C for the compounds investigated. For example, 1-NpSiPh(OH)$_2$ showed no significant aryl cleavage at 150 °C, but at 180 °C (Figures S31 and S32). The aryl cleavage in silanediols also leads to the formation of T-units (three oxygen atoms bound at one silicon atom), which could also be detected for some compounds in the distillation sump via ^{1}H-^{29}Si HMBC NMR spectroscopy (Figures S33 and S34). The formation of Q-units (four oxygen atoms bound at one silicon atom), could not be detected. We were also able to prove that this aryl cleavage can similarly occur in monosilanols (Figure S35–S39), giving rise to difunctional units like dimethylsiloxanes as described above. Higher temperatures are not the only requirement for aryl cleavage; the presence of nucleophilic groups, for example silanol groups, is also necessary.[70–71]

For a comparative quantification of the cleavage, a temperature of 180 °C and a condensation time of 4 h were chosen for all compounds. The corresponding NMR spectra can be found in the supporting information (Figures S40–S43). The amount of the cleaved molecules obtained by integration in the ^{1}H spectrum and integration of the reference substance was put in relation to the amount of substance from the corresponding silanediol. This value is plotted in Figure 6. Based on the amount of water molecules detected, it can be shown that diphenylsilanediol (Ph$_2$Si(OH)$_2$) has the highest degree of condensation under these conditions, followed by 1-NpSiMe(OH)$_2$ and 1-NpSiPh(OH)$_2$, which have a similar degree of condensation. 9-PheSiPh(OH)$_2$ exhibits the lowest degree of condensation with an elimination of 20% water, based on the total molecule. The benzene cleavage of the phenyl-containing molecules decreases within the series from about 20% for Ph$_2$Si(OH)$_2$ to less than 1% for 9-PheSiPh(OH)$_2$. In contrast, the polycyclic aromatics show a higher tendency to cleave from the siloxane backbone than the phenyl groups in the same molecule. This is 15% Naphthyl / 2% Phenyl for 1-NpSiPh(OH)$_2$ and 12% Phenanthrenyl / 0.5% Phenyl for 9-PheSiPh(OH)$_2$.

Two mechanisms for the cleavage of organic substituents on silicon have generally been formulated in the literature.[70–73] The oxidative cleavage of the substituents can be eliminated here based on the experimental conditions and the condensation products found. The other possible route to substituent cleavage occurs via nucleophilic substitution at the silicon atom.[71,73] The nucleophile can theoretically be an intermediate water molecule or an active silanol group. The result is the

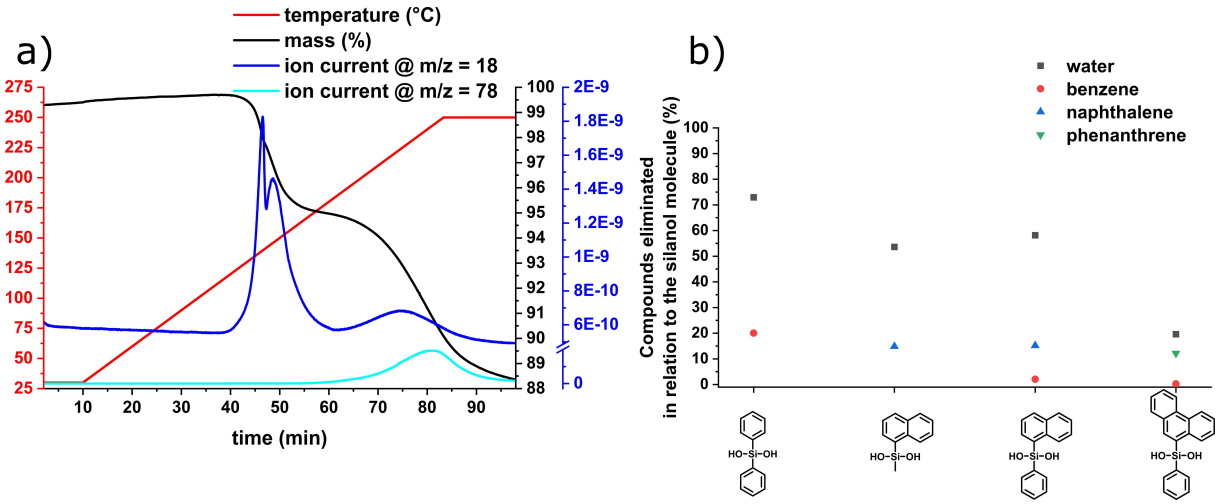

Figure 6. a) TG-MS measurement (30 – 250 °C with 3 K/min and isothermal segments at the beginning and at the end) of compound Ph$_2$Si(OH)$_2$, where water and benzene were tracked by MS b) Quantitative evaluation of volatile condensation products at a condensation temperature of 180 °C and a condensation time of 4 h.

same, with the subsequent hydroxyl group at the T^2 unit (–O_2Si-OH) (Scheme 4). Here it is debatable which nucleophile attacks. There are some arguments for and against water as a nucleophile. This issue was also debated in the literature, with hydrolysis by water being the predominant opinion.[71,73] However, Schott and Sprung provided convincing arguments for the attack of the silanol group, i.e. mechanism 1 (Scheme 4). Both energetic principles and experimental data argued against an attack of water in the studies.[70,72] As can be seen in Scheme 4, mechanism 1 can occur more frequently when the molecules or the functional groups are located very close to each other. This suggests that aryl cleavage by mechanism 1 occurs preferentially during condensation in substance or in the solid-state.

Structural properties of the resulting polysiloxanes

When investigating a possible thermal condensation in the solid-state, an investigation of the structure of the resulting condensation products in comparison to the original precursor in the solid-state is very interesting, because a possibly topotactic reaction can open a route to produce stereoregular polymers by solid-state condensation reactions.

In solid, crystalline form, silanediols often form hydrogen bond networks with different patterns. It can be expected that the hydrogen bonding patterns form reaction pathways for the condensation due to the orientation and spatial proximity. Hence, it is possible that the orientation of the original crystal structure is partially preserved in the condensation products. To test this hypothesis and to study the condensation processes in the crystalline solid, they were followed via repeated PXRD measurements at elevated temperatures. If a temperature well below the melting point is chosen for the solid condensation the structure of the resulting condensation products should be very similar to the structure of the precursor, while at temperatures above the melting point a relaxation of the structure can occur.

Diphenylsilandiol ($Ph_2Si(OH)_2$)

$Ph_2Si(OH)_2$ shows a transformation of the highly crystalline solid with defined reflections to a material (Figure 7) exhibiting only two very broad reflections at 8.2 and 18.8° 2θ. As visible in the previous studies, the condensation conditions used at this stage showed a relatively low condensation progress (about 25% of the silanol groups and 10% of the $Ph_2Si(OH)_2$ are consumed (Figure 1 and Figure 2)), but no changes after 35 min are visible.

However, the two very broad reflections are often interpreted in literature as ordering phenomena in polysiloxanes.[74–76] For ladder-like systems the two broad reflections were assigned to chain and intrachain spacing,[75] or the ladder width and thickness.[74,76] Using the Bragg equation, the distances associated with these reflections can be determined. For $Ph_2Si(OH)_2$, the two broad reflections could be correlated with structural elements of the distances 0.47 nm and 1.08 nm (Figure 8a).

If we try to correlate the distances found in the PXRD measurements with those of the single crystal of diphenylsilanediol (Figure 8b), we can conclude that the larger distance of 1.09 nm corresponds to the distance between the "pillars" in the crystal structure of $Ph_2Si(OH)_2$, which are formed by the hydrogen bonds (Figure 8b). The smaller distance of 0.47 nm can be attributed to the diameter of the columns. Therefore, it is assumed that the superordinate structure was preserved, and the condensation took place exclusively in the *c*-direction. The amorphization of the material can be explained by the possible rotational processes of the organic substituents. The phenyl rings, for example, would have to undergo a strong rotation due to the condensation of the silanol groups in the *c*-direction alone and the associated changes in the bond angles.

As mentioned above, $Ph_2Si(OH)_2$ was measured at two different temperatures. The temperatures were chosen so that one temperature was well below the melting point to ensure an actual solid-state condensation and the other temperature was above the melting point. The hypothesis here was a possible structural change in the resulting condensation

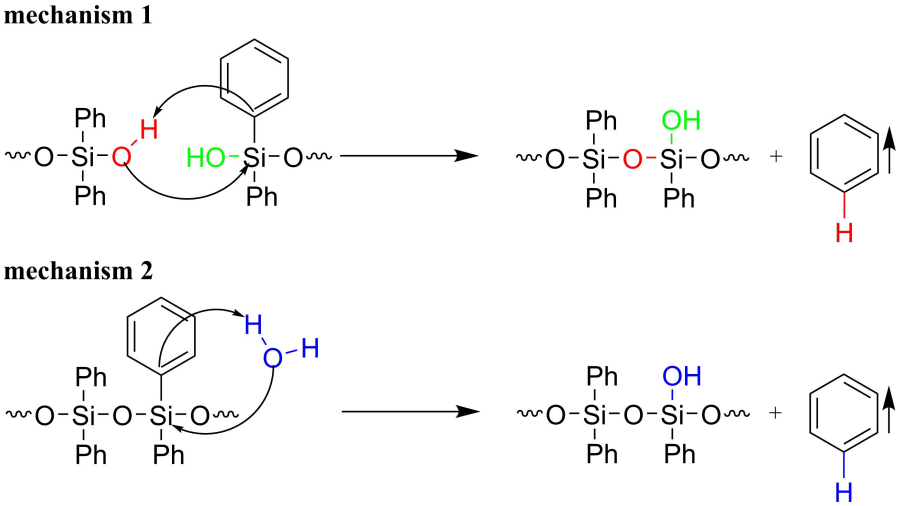

Scheme 4. Schematic representation of the two mechanisms postulated here in the thermal cleavage of phenyl groups.

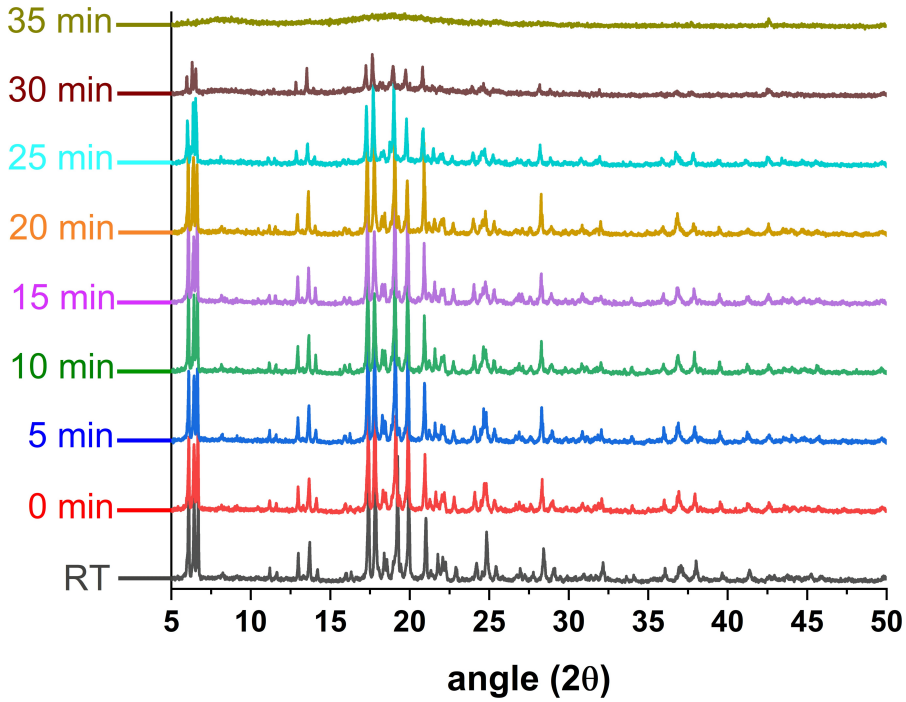

Figure 7. Time dependent powder X-ray diffractograms of $Ph_2Si(OH)_2$ at 130 °C with a first measurement at room temperature.

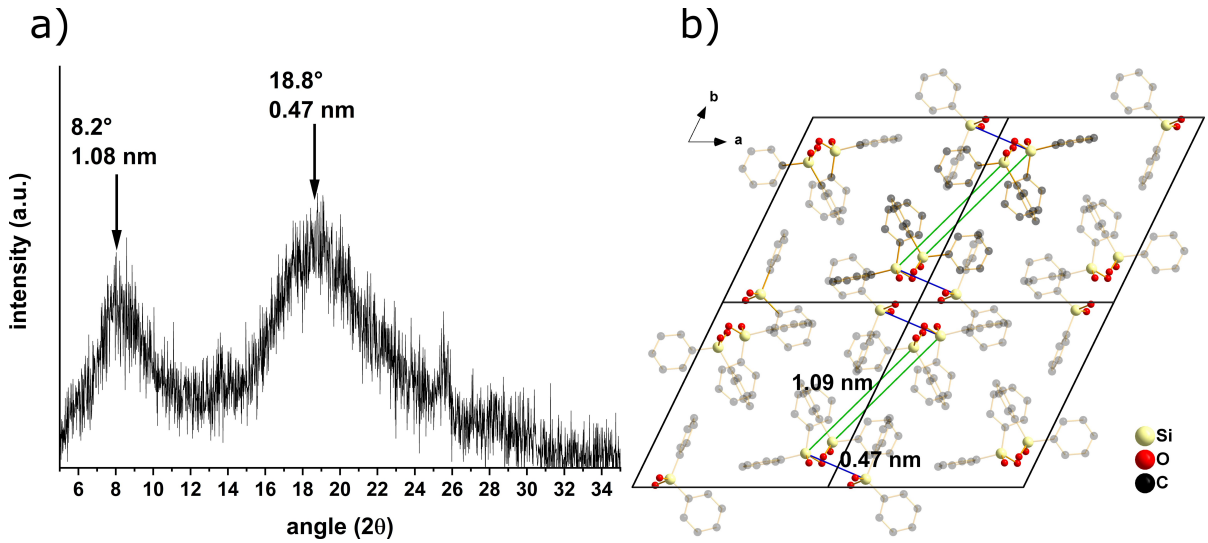

Figure 8. a) Powder X-ray diffractogram of the resulting material from heating the silanediol $Ph_2Si(OH)_2$ at 130 °C. The two reflections at 8.2° and 18.8° 2θ were observed, which corresponds to distances of 1.08 nm and 0.47 nm. b) Single crystal structure of the silanol $Ph_2Si(OH)_2$ with marked distances. For the sake of clarity, the two phenyl groups on each silicon atom have been shown only in a transparent manner. The direction of view along [001] goes through the pillars.

product due to the elevated temperature and the associated change in aggregate state. In the case of the diphenylsilanediol ($Ph_2Si(OH)_2$) studied here, no difference in the structure of the condensed species was observed. This could be due to several reasons: although the sample was heated very quickly to the measurement temperature in the reaction chamber of the PXRD instrument, it would be possible that the solid-state condensation as a structure-giving process occurs so quickly that it is already almost completed before the substance melts. Another possible explanation would be that it makes no difference whether the silanol condenses in the solid or in the melt, since the resulting species arrange themselves by self-assembly phenomena in a very similar structure to the crystalline silanol.

1,3-Dihydroxy-1,1,3,3-tetraphenyldisiloxane is the first condensation product in the condensation of diphenylsilanediol ($Ph_2Si(OH)_2$). For this reason, a comparison of the crystalline structure[77–79] is helpful and useful. However, the comparison of the powder diffractograms of the disiloxane and the diphenylsi-

lanediol after 20 min at 130 °C (Figure 7) shows no similarities. The powder diffractograms in Figure 7 only show reflections of the starting compound ($Ph_2Si(OH)_2$), which become smaller during condensation. It is conceivable that compounds formed during condensation are not present in crystalline form and are therefore not visible in the powder diffractogram. When looking at the single crystal structure, it is noticeable that the hydrogen-bridged pillar-like structural motifs, which can be seen in diphenylsilanediol (Figure 8 b and Figure S6), can also be seen in its dimer. This supports the hypothesis of a condensation of the hydrogen bonds while retaining the basic structure.

1-Naphthylmethylsilandiol (1-NpSiMe(OH)$_2$)

Very poor data were repeatedly obtained in the single crystal structure analysis of 1-NpSiMe(OH)$_2$. The reason for this is that there are many layers growing on top of each other, resulting in a multiple twinned system. For this reason, this crystal structure was not registered in the cambridge structural database. The structural data from the single crystal structure were therefore refined and improved with the help of powder XRD data. However, the connectivities were clearly visible, which makes a discussion of the general structure appropriate. The reason for these problems is also the layered structure of 1-NpSiMe(OH)$_2$ in the solid-state. Here, the silanol groups form a two-dimensional arrangement through hydrogen bonds, with the substituents (1-naphthyl + methyl) orthogonal to this plane. After thermally induced solid-state condensation, two broad reflections are observed in the PXRD (Figure 9a). The reflection at 20.5° 2θ can be assigned to a spacing within the bridged planes (0.43 nm, Figure 9b).

At smaller angles (about 11° 2θ) an even broader reflection is observed, which corresponds to a distance of about 0.6–0.8 nm. In the crystal structure of the reactant (1-NpSiMe(OH)$_2$) it is noticeable that the different distances of silicon atoms between the planes are between 1.2 and 1.6 nm (Figure 10). These distances agree with the very broad reflection in the PXRD of the condensed species when considering them to be double in length. As mentioned above, the substance was condensed both below its melting point (110 °C) and above its melting point (140 °C) of mp = 130 °C. As with $Ph_2Si(OH)_2$, the condensation products do not differ from each other in PXRD patterns. Thus, the structure seems to evolve independently of the state of aggregation during condensation.

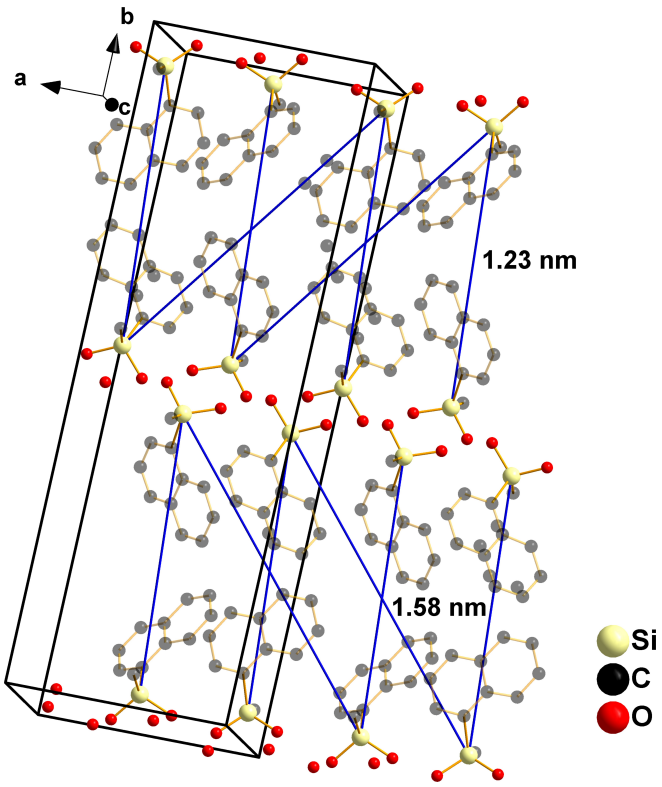

Figure 10. Parallel view of the hydrogen bond linked planes of 1-NpSiMe(OH)$_2$ with highlighting of the distances found in the PXRD. For the sake of clarity, the two aryl groups on each silicon atom have been shown only in a transparent manner.

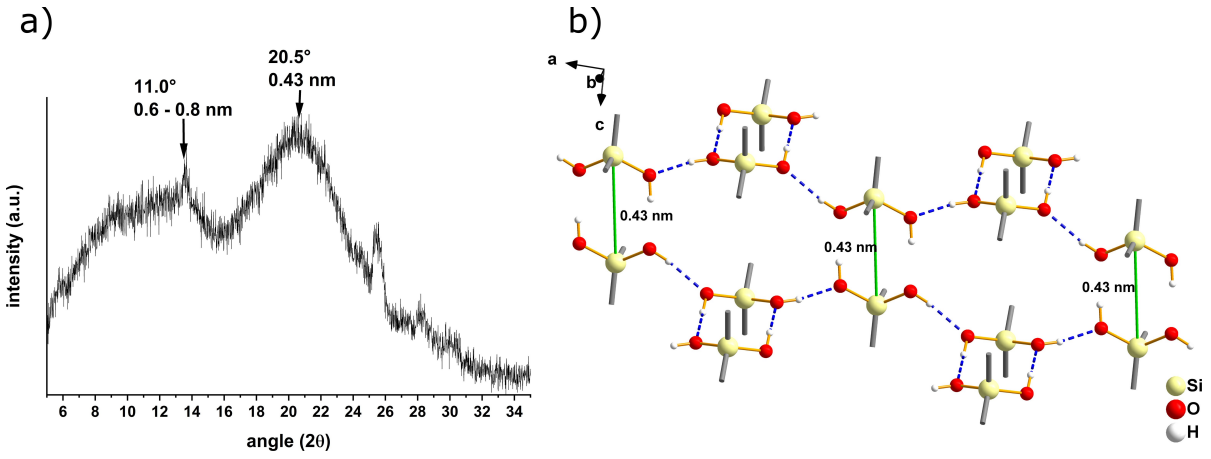

Figure 9. a) Powder X-ray diffractogram of the resulting material from heating the silanol 1-NpSiMe(OH)$_2$ at 110 °C. The two reflections were at about 11 and 20.5° 2θ, which corresponds to 0.6–0.8 nm and 0.43 nm. b) Orthogonal view of the hydrogen bond linked planes of compound 1-NpSiMe(OH)$_2$ with highlighting of the distances found in the SCXRD. The substituents have only been implied here by their bonds, for the sake of clarity.

1-Naphthylphenylsilandiol (1-NpSiPh(OH)$_2$)

The powder X-ray diffractograms of the synthesized 1-NpSiPh(OH)$_2$ were compared with the three available single crystal structures (1-NpSiPh(OH)$_2$·1/3 H_2O; 1-NpSiPh(OH)$_2$·1/3 CH_3OH; 1-NpSiPh(OH)$_2$·1/4 CH_2Cl_2) to determine the most structurally similar structure. It was found that the structure with additional water molecules was most comparable to the compound observed immediately after synthesis.

The structure of 1-NpSiPh(OH)$_2$ is mainly characterized by hexamers. Within these hexamers, two distances, i.e., 0.47 nm and 0.63 nm, can be identified from the X-ray diffraction patterns of the condensed species (Figure 11b). The spacing of approx. 1.2 nm is also found both in the single crystal structure of the silanediol and in the X-ray diffraction pattern of the condensed species (Figure 11a). Here, too, the basic structure seems to be preserved.

9-Phenanthrenylphenylsilandiol (9-PheSiPh(OH)$_2$)

9-PheSiPh(OH)$_2$ does not show a distinct hydrogen bond network due to its large aryl substituents, but it forms hydrogen bond supported tetramers. Because of the rather small aggregates, a structural investigation of the condensation product, especially in comparison to the infinite hydrogen bond networks of $Ph_2Si(OH)_2$ and 1-NpSiMe(OH)$_2$, is interesting. The PXRD study of the condensation product of the thermal condensation of 9-PheSiPh(OH)$_2$ showed only one broad reflection (Figure 12a). The maximum of this reflection corresponds to a distance of 0.49 nm. In the crystal structure of the corresponding silanediol, this distance can be found several times (Figure 12b).

The studied silanediols were examined by X-ray diffraction during thermal condensation. It was shown that the initially sharp and defined reflections of the crystalline silanediols disappear during condensation and very broad reflections are

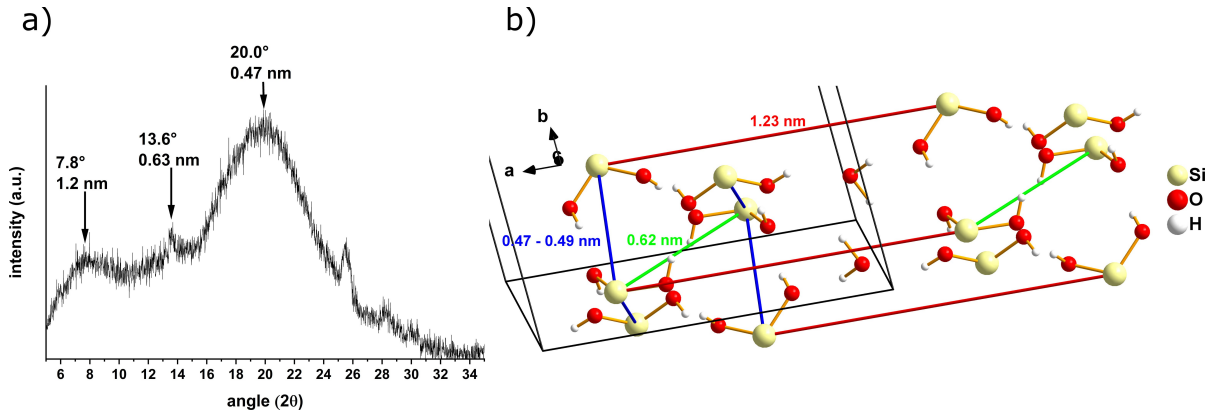

Figure 11. a) Powder X-ray diffractogram of the resulting material from heating 1-NpSiPh(OH)$_2$ at 125 °C. The three reflections were at 7.8, 13.6, and 20.0° 2θ which corresponds to 1.2, 0.63, and 0.47 nm, respectively. b) Crystal structure of 1-NpSiPh(OH)$_2$ with marked distances. The substituents are not shown here for clarity.

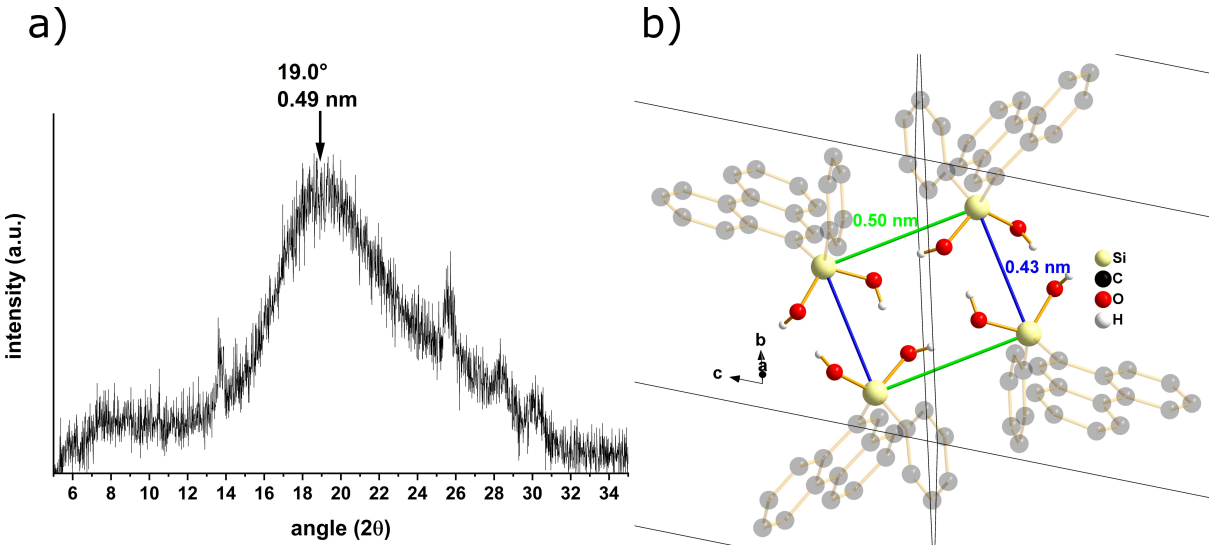

Figure 12. a) X-ray diffractogram of the resulting material from heating 9-PheSiPh(OH)$_2$ at 155 °C. The reflection at 19.0° 2θ corresponds to 0.49 nm. b) Crystal structure of 9-PheSiPh(OH)$_2$ with marked distances. For the sake of clarity, the two aryl groups on each silicon atom have been shown only in a transparent manner.

formed. In the case of 9-PheSiPh(OH)$_2$, one broad reflection could be identified, in the case of $Ph_2Si(OH)_2$ and 1-NpSiMe(OH)$_2$ two and in the case of 1-NpSiPh(OH)$_2$ three broad reflections could be identified. The position of the reflections could be associated to the intermolecular distances from the single crystal structure of the silanediols. Thus, it could be shown that the crystalline structure of the precursor molecules is at least partially conserved in the condensation products. There seems to be no difference between solid-state condensation, i.e. condensation below the melting point, and condensation in the melt.

Conclusions

The condensation behavior of diphenylsilanediol ($Ph_2Si(OH)_2$), 1-naphthylmethylsilandiol (1-NpSiMe(OH)$_2$), 1-naphthylphenylsilanediol (1-NpSiPh(OH)$_2$) and 9-phenanthrenylphenylsilanediol (9-PheSiPh(OH)$_2$) was investigated. Diphenylsilanediol was studied extensively due to its importance in many processes. As expected, the rate of condensation increased with increasing temperature and time, with compound $Ph_2Si(OH)_2$ condensing well below the melting point. The influence of the substitution pattern was basically shown by a slower reaction with sterically larger substituents in the compounds 1-NpSiPh(OH)$_2$ and 9-PheSiPh(OH)$_2$. However, aryl cleavage was also observed here, which again complicates the comparison. Thermogravimetric investigations of the silanediol condensation supported the condensation kinetics from the NMR study. With respect to molar mass all samples showed rather small chain lengths of about 2–8 units as analyzed by SEC. As expected, longer condensation times result in increasing molar masses of the (oligo)siloxanes. FT-ICR MS measurements confirmed the results from SEC. Also, the T_g increased with increasing condensation time and temperature, as well as with the increasing steric demand of the substituents on the silicon atom. Aryl group cleavage seems to be a major problem in the thermal condensation reactions particularly at higher temperatures. Cleavages of up to 20 mol% for phenyl substituents ($Ph_2Si(OH)_2$), 15 mol% for naphthyl substituents and 12 mol% for phenanthrenyl substituents were detected. The cleavage mechanism involves a nucleophilic attack of silanol groups on the silicon and the concomitant cleavage of the substituents. Structural studies of the condensation products were realized by in situ PXRD studies during thermal condensation of the silanediols. All condensation products showed one to three very broad reflections, which could be correlated with specific distances within the single crystal structures of the silanediols used. From this it can be concluded that the original crystal structure is partially preserved, whereby it can be assumed that the thermal condensation is influenced or even directed by the pre-orientation of the hydrogen bonds. Thus a topotactic reaction control is probable.

Supporting Information

The authors have cited additional references within the Supporting Information.[11,67, 80–85]

Acknowledgements

Instrumentation and technical assistance for this work were provided by the Service Center X-ray Diffraction, with financial support from Saarland University and German Science Foundation (project numbers INST 256/506-1, INST 256/349-1) and by the Service Center NMR at UdS, with financial support from Saarland University and German Science Foundation DFG. We want to thank Blandine Boßmann and Frank Hartmann for the measurement and evaluation of the SEC investigations at the Institute of Polymer Chemistry and we want to thank Dr. Klaus Hollemeyer for the MALDI measurements and data evaluation. Open Access funding enabled and organized by Projekt DEAL.

Conflict of Interests

The authors declare no conflict of interest.

Data Availability Statement

The data that support the findings of this study are available in the supplementary material of this article.

Keywords: Organosilanols · solid-state condensation · solid-state polymerization · thermal analysis

[1] K. Zalewski, Z. Chylek, W. A. Trzcinski, *Polymer* **2021**, *13*, 1–11.
[2] J. Y. Bae, Y. Kim, H. Kim, Y. Kim, J. Jin, B. S. Bae, *ACS Appl. Mater. Interfaces* **2015**, *7*, 1035–1039.
[3] J. Chen, Z. Fu, H. Huang, X. Zeng, Z. Chen, *RSC Adv.* **2016**, *6*, 71924–71933.
[4] M. Zhao, Y. Feng, G. Li, Y. Li, Y. Wang, Y. Han, X. Sun, X. Tan, *Polym. Adv. Technol.* **2014**, *25*, 927–933.
[5] X. Yang, Q. Shao, L. Yang, X. Zhu, X. Hua, Q. Zheng, G. Song, G. Lai, *J. Appl. Polym. Sci.* **2013**, *127*, 1717–1724.
[6] Z. Ren, S. Yan, *Prog. Mater. Sci.* **2016**, *83*, 383–416.
[7] F. D. Osterholtz, E. R. Pohl, *J. Adhes. Sci. Technol.* **1992**, *6*, 127–149.
[8] J. A. Semlyen, in *Adv. Polym. Sci.* **1976**.
[9] K. Licht, H. Kriegsmann, *Z. Anorg. Allg. Chem.* **1963**, *323*, 252–259.
[10] P. D. Lickiss, in *Adv. Inorg. Chem., Vol. 42* (Ed.: A. G. Sykes), **1995**, pp. 147–262.
[11] J. F. Kannengiesser, M. Briesenick, D. Meier, V. Huch, B. Morgenstern, G. Kickelbick, *Chem. Eur. J.* **2021**, *27*, 16461–16476.
[12] S. Bilda, G. Röhr, D. Lange, E. Popowski, H. Kelling, *Z. Anorg. Allg. Chem.* **1988**, *564*, 155–160.
[13] W. T. Grubb, *J. Am. Chem. Soc.* **1954**, *76*, 3408–3414.
[14] G. F. L. Ehlers, K. R. Fisch, *Air Force Materials Laboratory* **1975**.
[15] V. P. Privalko, Y. S. Lipatov, *J. Macromol. Sci., Part B: Phys.* **1974**, *9*, 551–564.
[16] K. E. Polmanteer, M. J. Hunter, *J. Appl. Polym. Sci.* **1959**, *1*, 3–10.
[17] E. Pérez, A. Bello, J. M. Pereña, *Polym. Bull.* **1988**, *20*, 291–296.
[18] X. Yu, J. Jia, S. Xu, K. U. Lao, M. J. Sanford, R. K. Ramakrishnan, S. I. Nazarenko, T. R. Hoye, G. W. Coates, R. A. DiStasio, *Nat. Commun.* **2018**, *9*, 1–9.
[19] D. Meier, V. Huch, G. Kickelbick, *J. Polym. Sci.* **2021**, *59*, 2265–2283.

[20] M. Briesenick, M. Gallei, G. Kickelbick, *Macromolecules* **2022**, *55*, 4675–4691.
[21] O. Nillius, H. Kriegsmann, *Spectrochim. Acta Part A* **1970**, *26 A*, 121–130.
[22] J. Beckmann, D. Dakternieks, A. Duthie, M. L. Larchin, E. R. T. Tiekink, *Appl. Organomet. Chem.* **2003**, *17*, 52–62.
[23] J. F. Hyde, *J. Am. Chem. Soc.* **1953**, *75*, 2166–2167.
[24] J. Fawcett, R. June, *Can. J. Chem.* **1977**, *55*, 3631–3635.
[25] N. H. Buttrus, C. Eaborn, P. B. Hitchcock, P. D. Lickiss, A. D. Taylor, *J. Organomet. Chem.* **1986**, *309*, 25–33.
[26] S. S. Al-Juaid, C. Eaborn, P. B. Hitchcock, P. D. Lickiss, *J. Organomet. Chem.* **1989**, *362*, 17–22.
[27] N. H. Buttrus, C. Eaborn, P. B. Hitchcock, P. D. Lickiss, *J. Organomet. Chem.* **1986**, *302*, 159–163.
[28] L. J. Tyler, *J. Am. Chem. Soc.* **1955**, *77*, 770–771.
[29] H. Ishida, J. L. Koenig, K. C. Gardner, *J. Chem. Phys.* **1982**, *77*, 5748–5751.
[30] H. Ishida, J. L. Koenig, *Appl. Spectrosc.* **1978**, *32*, 469–479.
[31] N. Winkhofer, H. W. Roesky, M. Noltemeyer, W. T. Robinson, *Angew. Chem. Int. Ed. Engl.* **1992**, *31*, 599–601.
[32] M. W. Mutahi, T. Nittoli, L. Guo, S. M. Sieburth, *J. Am. Chem. Soc.* **2002**, *124*, 7363–7375.
[33] C. A. Chen, S. M. N. Sieburth, A. Glekas, G. W. Hewitt, G. L. Trainor, S. Erickson-Viitanen, S. S. Garber, B. Cordova, S. Jeffry, R. M. Klabe, *Chem. Biol.* **2001**, *8*, 1161–1166.
[34] S. E. Denmark, A. Ambrosi, *Org. Process Res. Dev.* **2015**, *19*, 982–994.
[35] S. E. Denmark, R. F. Sweis, *Acc. Chem. Res.* **2002**, *35*, 835–846.
[36] K. Hirabayashi, Y. Nishihara, A. Mori, T. Hiyama, *Tetrahedron Lett.* **1998**, *39*, 7893–7896.
[37] D. C. Braddock, B. C. Rowley, P. D. Lickiss, S. J. Fussell, R. Qamar, D. Pugh, H. S. Rzepa, A. J. P. White, *J. Org. Chem.* **2023**, *88*, 9853–9869.
[38] V. Chandrasekhar, R. Boomishankar, S. Nagendran, *Chem. Rev.* **2004**, *104*, 5847–5910.
[39] R. Murugavel, V. Chandrasekhar, H. W. Roesky, *Acc. Chem. Res.* **1996**, *29*, 183–189.
[40] S. Spirk, M. Nieger, R. Pietschnig, *Dalton Trans.* **2009**, *596*, 163–167.
[41] R. Pietschnig, S. Spirk, *Coord. Chem. Rev.* **2016**, *323*, 87–106.
[42] N. Hurkes, C. Bruhn, F. Belaj, R. Pietschnig, *Organometallics* **2014**, *33*, 7299–7306.
[43] E. Miller, I. Fankuchen, H. Mark, *J. Appl. Phys.* **1949**, *20*, 531–533.
[44] H. Morawetz, S. Z. Jakabhazy, J. B. Lando, J. Shafer, *Proc. Natl. Acad. Sci. USA* **1963**, *49*, 789–793.
[45] R. Srinivasan, P. Desai, A. S. Abhiraman, R. S. Knorr, *J. Appl. Polym. Sci.* **1994**, *53*, 1731–1743.
[46] G. Wegner, *Pure Appl. Chem.* **1977**, *49*, 443–454.
[47] H. Morawetz, *J. Polym. Sci. Part C* **1966**, *12*, 79–88.
[48] Z. Lasocki, S. Chrzczonowicz, *J. Polym. Sci.* **1962**, *59*, 259–269.
[49] S. D. Korkin, M. I. Buzin, E. V. Matukhina, L. N. Zherlitsyna, N. Auner, O. I. Shchegolikhina, *J. Organomet. Chem.* **2003**, *686*, 313–320.
[50] J. F. Brown Jr., *J. Am. Chem. Soc.* **1965**, *87*, 4317–4324.
[51] N. Winkhofer, A. Voigt, H. Dorn, H. W. Roesky, A. Steiner, D. Stalke, A. Reller, *Angew. Chem. Int. Ed. Engl.* **1994**, *33*, 1352–1354.
[52] K. F. Bowes, C. Glidewell, J. N. Low, *Acta Crystallogr. Sect. C* **2002**, *58*, o409-o415.
[53] S. M. Barry, H. Mueller-Bunz, P. J. Rutledge, *Acta Crystallogr. Sect. E* **2008**, *64*, o1174.
[54] J. Beckmann, A. Duthie, G. Reeske, M. Schürmann, *Organometallics* **2004**, *23*, 4630–4635.
[55] S. A. Bourne, L. R. Nassimbeni, K. Skobridis, E. Weber, *J. Chem. Soc. Chem. Commun.* **1991**, 282–283.
[56] A. J. Lough, D. E. Turkington, G. Ferguson, C. Glidewell, *Acta Crystallogr. Sect. B* **2004**, *60*, 238–248.
[57] H. Puff, K. Braun, H. Reuter, *J. Organomet. Chem.* **1991**, *409*, 119–129.
[58] H. W. Lerner, S. Scholz, N. Wiberg, K. Polborn, M. Bolte, M. Wagner, *Z. Anorg. Allg. Chem.* **2005**, *631*, 1863–1870.
[59] M. Söderholm, *Acta Chem. Scand. Ser. B* **1984**, *38*, 31–35.
[60] M. E. Belowich, J. M. Roberts, T. H. Peterson, E. Bellinger, K. Syverud, T. Sidle, *Macromolecules* **2020**, *53*, 7487–7495.
[61] L. Tong, Y. Feng, X. Sun, Y. Han, D. Jiao, X. Tan, *Polym. Adv. Technol.* **2018**, *29*, 2245–2252.
[62] M. Zhao, Y. Feng, Y. Li, G. Li, Y. Wang, Y. Han, X. Sun, X. Tan, *J. Macromol. Sci., Part A: Pure Appl. Chem.* **2014**, *51*, 653–658.
[63] J. S. Kim, S. Yang, B. S. Bae, *Chem. Mater.* **2010**, *22*, 3549–3555.
[64] M. Chen, G. Zhang, X. Liang, W. Zhang, L. Zhou, B. He, P. Song, X. Yuan, C. Zhang, L. Zhang, H. Yu, H. Yang, *RSC Adv.* **2016**, *6*, 70825–70831.
[65] S. Yang, S.-Y. Kwak, J. Jin, J.-S. Kim, Y. Choi, K.-W. Paik, B.-S. Bae, *J. Mater. Chem.* **2012**, *22*.
[66] Y. H. Kim, J. Y. Bae, J. Jin, B. S. Bae, *ACS Appl. Mater. Interfaces* **2014**, *6*, 3115–3121.
[67] D. J. Neal, R. D. Blaumanis, *Anal. Chem.* **1960**, *32*, 139.
[68] W. J. Malfait, W. E. Halter, R. Verel, *Chem. Geol.* **2008**, *256*, 269–277.
[69] V. N. Novikov, E. A. Rössler, *Polymer* **2013**, *54*, 6987–6991.
[70] G. Schott, W. D. Sprung, *Z. Anorg. Allg. Chem.* **1964**, *333*, 76–89.
[71] R. Müller, L. Klenk, *J. Prakt. Chem.* **1955**, *4*, 129–152.
[72] K. Damm, W. Noll, *Kolloid-Z.* **1958**, *158*, 97–108.
[73] G. Schott, H. Berge, *Z. Anorg. Allg. Chem.* **1958**, *297*, 32–43.
[74] X. Zhang, L. Shi, C. Huang, *Chin. J. Polym. Sci.* **1987**, *5*, 353–358.
[75] L. A. S. D. A. Prado, E. Radovanovic, H. O. Pastore, I. V. P. Yoshida, I. L. Torriani, *J. Polym. Sci. Part A* **2000**, *38*, 1580–1589.
[76] K. Deng, T. Zhang, X. Zhang, A. Zhang, P. Xie, R. Zhang, *Macromol. Chem. Phys.* **2006**, *207*, 404–411.
[77] V. E. Shklover, Y. T. Struchkov, I. V. Karpova, V. A. Odinets, A. A. Zhdanov, *Zh. Strukt. Khim.* **1985**, *26*, 125–122.
[78] R. Shankar, N. Mahavar, *Dalton Trans.* **2020**, *49*, 16633–16637.
[79] M. A. Hossain, M. B. Hursthouse, *J. Crystallogr. Spectrosc. Res.* **1988**, *18*, 227–234.
[80] G. M. Sheldrick, *Acta Crystallogr.* **2015**, *C71*, 3–8.
[81] G. M. Sheldrick, *Acta Crystallogr.* **2015**, *A71*, 3–8.
[82] C. B. Hübschle, G. M. Sheldrick, B. Dittrich, *J. Appl. Crystallogr.* **2011**, *44*, 12811284.
[83] Topas 5, Bruker AXS, Karlsruhe, Germany, **2014**.
[84] P. Voss, C. Meinicke, E. Popowski, H. Kelling, *J. Prakt. Chem.* **1978**, *320*, 34–42.
[85] T. J. Kistenmacher, M. Rossi, L. K. Frevel, *J. Appl. Crystallogr.* **1978**, *11*, 670–671.

Manuscript received: October 11, 2023
Accepted manuscript online: December 26, 2023
Version of record online: February 2, 2024